RSC Advances

PAPER

View Article Online
View Journal | View Issue

Cite this: *RSC Adv.*, 2024, **14**, 15408

Detection of epinephrine using a $K_2Fe_4O_7$ modified glassy carbon electrode†

Mingcheng Jiang, Decheng Zeng, Xinxin Zheng and Hongming Yuan *

Received 10th January 2024
Accepted 4th May 2024

DOI: 10.1039/d4ra00242c

rsc.li/rsc-advances

Iron-based electrochemical catalysts used to modify electrodes for biosensing have received more attention from biosensor manufacturers because of their excellent biocompatibility and low cost. In this work, a fast-ion conductor potassium ferrite ($K_2Fe_4O_7$) modified glassy carbon electrode (GCE) was prepared for detecting epinephrine (EP) by electrochemical techniques. The obtained $K_2Fe_4O_7$/GCE electrode exhibited not only a wide linear range over EP concentration from 2 μM to 260 μM with a detection limit of 0.27 μM (S/N = 3) but also high selectivity toward EP in the presence of common interferents ascorbic acid (AA) and uric acid (UA), as well as good reproducibility and stability.

Introduction

Epinephrine (EP), $C_9H_{13}NO_3$ [(*R*)-4-(1-hydroxy-2-[methylamin] ethyl) benzene-1,2-diol], is a vital neurotransmitter belonging to the catecholamine group in the central nervous system of mammals.[1] In pharmaceutical applications, EP has been utilized to treat various conditions such as myocardial infarction, bronchial asthma, Parkinson's disease, and hypertension.[2,3] The multifaceted effects of EP include cardiovascular and cerebrovascular constriction, augmentation of heart activity, and elevation of blood pressure.[4] These ailments are closely associated with the concentration levels of EP in the human body. Accurate detection of EP in biological fluids like blood and urine holds immense significance.[5]

Several quantitative analytical methods have been established to determine EP concentrations, such as high-performance liquid chromatography (HPLC),[6] fluorimetry,[7] and electrochemiluminescence.[8] Since EP is an electroactive molecule, electrochemical techniques have emerged as practical and cost-effective approaches.[9] Electrochemical sensors utilizing glassy carbon electrodes (GCE) and carbon paste electrodes have been commonly employed for EP detection. To enhance their performance, various materials, such as organic molecules,[10] polymers[11], carbon nanotubes[12], graphene[13], and precious metals[14], have been explored as catalysts to modify the bare electrodes, resulting in improved electrocatalytic activity for EP.

Iron, the fourth most abundant element in the Earth's crust, has garnered considerable attention for its catalytic properties, particularly iron oxides.[15] Iron is also integral to biomolecules such as hemoglobin and myoglobin. Consequently, iron-containing materials have shown promise in biosensor applications. Recent studies have successfully detected dopamine (DA), another catecholamine neurotransmitter, using electrodes modified with iron oxide nanoparticles,[16–18] Fe-based metal–organic frameworks (MOFs),[19] and cobalt-doped $FePS_3$.[20] However, no reported electrode is modified by iron-based materials that demonstrate electrocatalytic activity for the oxidation of EP.

$K_2Fe_4O_7$, a compound displaying superionic conducting properties, is particularly favorable for enhancing the transfer ability of electrons. Our research group has previously reported successfully applying a $K_2Fe_4O_7$-modified GCE electrode to determine DA.[21] Building on this, we explore the electrocatalytic activity of the $K_2Fe_4O_7$/GCE electrode towards the oxidation of EP in this work. Furthermore, we investigate the performance of the electrode in detecting EP in the presence of interfering substances, such as ascorbic acid (AA) and uric acid (UA). The reproducibility and stability of the EP sensor are also evaluated.

Materials and methods

Materials

Epinephrine (EP) (99%), uric acid (UA) (99%), and ascorbic acid (AA) (99%) were bought from Sigma-Aldrich (Shanghai, China). Fe $(NO_3)_3 \cdot 9H_2O$, KOH, KH_2PO_4, HCl, and K_2HPO_4, were purchased from Sinopharm Chemical Reagent. Co. (China). All chemicals were analytical grade and used without any treatment. The phosphate buffer solution (PBS, 0.1 M) was prepared with K_2HPO_4 and KH_2PO_4, and the pH value ranging from 6.0 to 7.8 was adjusted by changing the radio of K_2HPO_4 and KH_2PO_4. Aqueous solutions used in experiments were prepared using deionized water with a resistance of 18.5 MΩ cm^{-1} obtained from an ultrapure water system (Wotepu, China).

State Key Laboratory of Inorganic Synthesis and Preparative Chemistry, College of Chemistry, Jilin University, Changchun, 130012, PR China. E-mail: hmyuan@jlu.edu.cn

† Electronic supplementary information (ESI) available. See DOI: https://doi.org/10.1039/d4ra00242c

Instruments and measurements

Powder X-ray diffraction (PXRD) experiments were measured on a Rigaku D-Max 2550 diffractometer (Rigaku, Japan) with Cu-Kα radiation (λ = 1.5418 Å). UV-Vis absorption spectra were collected with a UV-2450 spectrometer (Hitachi, Japan). All electrochemical measurements were tested at room temperature by CHI660C electrochemical workstation (Chenhua Co., Shanghai, China). Cyclic voltammetry (CV) and differential pulse voltammetry (DPV) were performed in a standard three-electrode system, which included bare and modified GCE as the working electrodes, Ag/AgCl/KCl (0.1 M) as the reference electrode, and platinum as the counter electrode.

Preparation of $K_2Fe_4O_7$

We acquired the single-phase crystalline $K_2Fe_4O_7$ through the hydrothermal method previously reported.[22] To ensure purity, the crystal surface was cleaned with 2.0 M HCl and washed several times with distilled water. After washing, the crystal was dried in a vacuum oven at 60 °C. The crystal was finally ground into a powder using a mortar for about one hour.

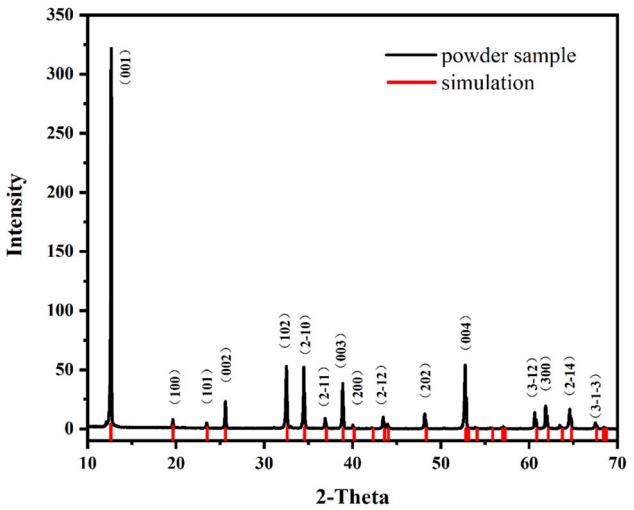

Fig. 1 The simulation and powder XRD patterns of $K_2Fe_4O_7$.

Construction of the modified electrode

The GCE (diameter = 3 mm) was polished with 0.05 μm alumina slurry. Afterward, the electrodes were ultrasonically cleaned in distilled water for 5 min and left to air dry at room temperature. The $K_2Fe_4O_7$ dispersion was prepared by adding 3 mg $K_2Fe_4O_7$ powder to a mixture of 5 mL dimethylformamide and 1 μL Nafion and then sonicating for 30 min. Take 10 μL of the dispersion at a time and drop it on the surface of the electrode, then let it dry naturally at room temperature and repeat three times until the $K_2Fe_4O_7$ is spread evenly over the surface of the electrode.

Results and discussion

Characterization of $K_2Fe_4O_7$

The crystal phase and purity of $K_2Fe_4O_7$ were confirmed through X-ray Diffraction analysis, as shown in Fig. 1. The results indicate that $K_2Fe_4O_7$ was successfully synthesized with a high purity level (Detailed crystal information is given in ESI S1†). Moreover, the samples obtained after grinding exhibited similarity to those identified through single crystal structure simulation. This observation suggests that the crystal structure of $K_2Fe_4O_7$ remained unchanged even after the grinding process.

The electrochemical response of EP

The electrochemical response of EP on the electrode surface and the electrocatalytic behavior of $K_2Fe_4O_7$ were investigated through the CV method. Initially, the bare electrode and $K_2Fe_4O_7$/GCE electrode were separately tested in PBS containing 100 μM EP. The CV results, as illustrated in Fig. 2(a), indicate that the response current of the $K_2Fe_4O_7$/GCE electrode was notably higher as compared to the bare electrode, thus indicating a considerable electrocatalytic effect of $K_2Fe_4O_7$ on EP. It is important to note that the CV plot clearly shows two sets of redox peaks. Specifically, A_1/B_1 corresponds to the redox process between adrenaline and adrenoquinone, and the relevant calculations in the testing process are based on the data from this oxidation peak unless otherwise specified. The other redox peaks represent the redox process between adrenochrome and

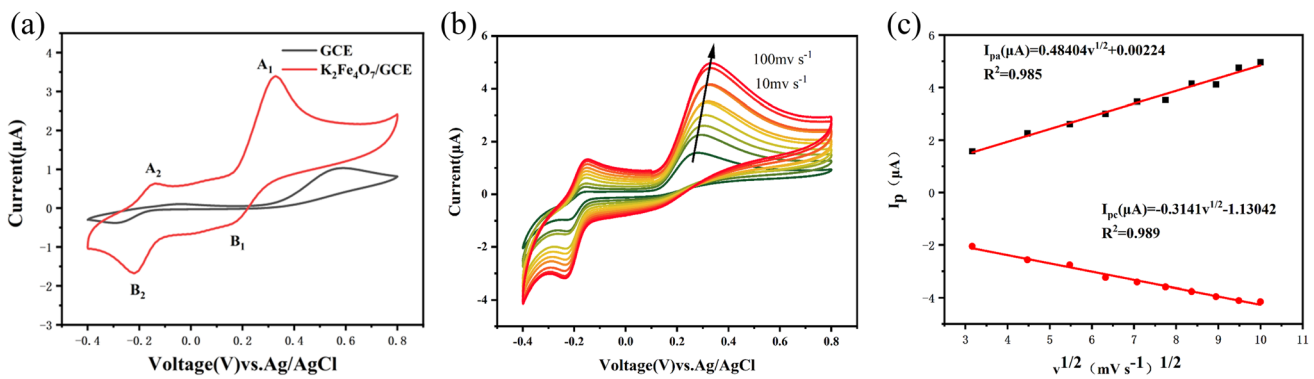

Fig. 2 (a) CV of bare GCE and $K_2Fe_4O_7$/GCE in 0.1 M PBS (pH = 7.4) containing 100 μM EP. (b) CVs of $K_2Fe_4O_7$/GCE in 0.1 M PBS (pH = 7.4) containing 100 μM EP at scan rates of 10–100 mV s^{-1}. (c) The plots of response currents and the square root of scan rate.

5,6-dihydroxy-*N*-methylindole[23] (Fig. S2†). The reason for the appearance of this specific pair of redox peaks is that $K_2Fe_4O_7$ has previously been demonstrated to be used as a catalyst for the oxygen evolution reaction. During the test, oxygen generation accompanies the oxidation of epinephrine to adrenochrome, resulting in a second pair of redox peaks. Additionally, the change in response current with scan rate can reflect the kinetic process of EP on the electrode surface. With a scan rate increase from 10 mV s^{-1} to 100 mV s^{-1}, there was a noticeable linear relationship between the response current and the square root of the scan rate, as shown in Fig. 2(b and c). This linearity proves that the redox process of EP is diffusion-controlled[24]

The effect of pH

To investigate the effect of pH on the performance of the electrochemical sensor for EP, PBS solutions with various pH values containing 100 μM EP were prepared and tested (Fig. 3(a)). The results showed that the response potential of the sensor displayed a linear decrease with the increase of pH, with a slope of approximately 0.052 mV pH^{-1}, indicating the transfer of two protons during the reaction.[25] The response current of the sensor increased with the pH value until it reached its maximum value at pH 7.4, after which it decreased with further increases in pH. As a result, pH 7.4 was determined to be the optimal pH value for the sensor (Fig. 3(a)). Subsequent experiments were conducted at this pH value unless otherwise specified.

Calibration curve

Differential pulse voltammetry (DPV) was employed as a highly responsive and rapid detection technique for adrenaline (EP). To establish the relationship between the response current and the concentration of EP, DPV scans were performed in phosphate-buffered saline (PBS) with varying concentrations of EP (Fig. 3(b and c)). The results revealed a robust linear correlation between the response current and EP concentration within the range of 2 μM to 260 μM. The equation for this relationship is I_p (μA) = 0.00848$C_{(EP)}$ (μM) + 0.2756, with an impressive coefficient of determination (R^2 = 0.998). Additionally, the limit of detection for this sensor was determined to be 0.27 μM (See S3† for specific LOD calculations). The comparative analysis presented in Table 1 demonstrates the successful development of an EP sensor compared with other previously published studies.

Table 1 Comparison of the EP sensors reported in the literature

Material	Linear range (μM)	LOD (μM)	Technique	Reference
sG/Pd/GCE	2–50	0.1	DPV	26
ZnO/MWCNTs/GCE	0.4–2.4	0.016	DPV	27
Ty/MWCNTs/GCE	0.6–100	0.51	DPV	28
CAP/MWCNT/GCE	50–1150	7.2	CA	29
Graphene/GCE	0.2–100	0.001	CV	30
P(L-Asp)/ERGO/GCE	0.1–110	0.025	SWV	31
This work	2–260	0.27	DPV	This work

Selectivity of the sensor

During the electrochemical quantification of EP using biosensors, interfering substances such as ascorbic acid (AA) and uric acid (UA) can affect the accuracy of the results.[32] The DPV method was employed to assess the selectivity of the $K_2Fe_4O_7$/GCE electrode towards EP. The electrochemical activity of AA and UA on the surface of the $K_2Fe_4O_7$/GCE electrode was investigated, as depicted in Fig. 4(a). Interestingly, it was observed that AA exhibited no detectable electrochemical response, and although urea showed a weak electrochemical response around 0.32 V, it did not affect the detection results. The results indicate the sensor's exceptional selectivity towards EP.

Repeatability and stability

$K_2Fe_4O_7$ has been demonstrated to be a viable material for electrochemical analysis. Maintaining good repeatability and stability is crucial for electrochemical sensors in the detection process. The modified electrode was subjected to 25 independent measurements in a buffering solution containing 100 μM EP to further validate its repeatability and stability as an electrochemical sensor. As shown in Fig. 4(b), the results exhibited a relative standard deviation of 2.92%. The electrochemical

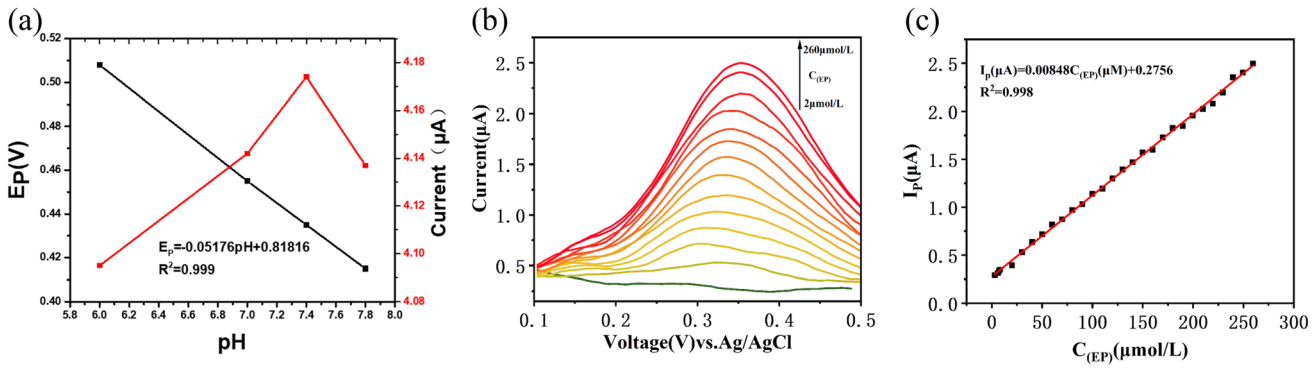

Fig. 3 (a) The plots of pH with response current and response potential in 0.1 M PBS containing 100 μM EP. (b) DPV of $K_2Fe_4O_7$/GCE for different EP concentrations in 0.1 M PBS (pH = 7.4). (c) Plots of the response current and EP concentrations (2–260 μM).

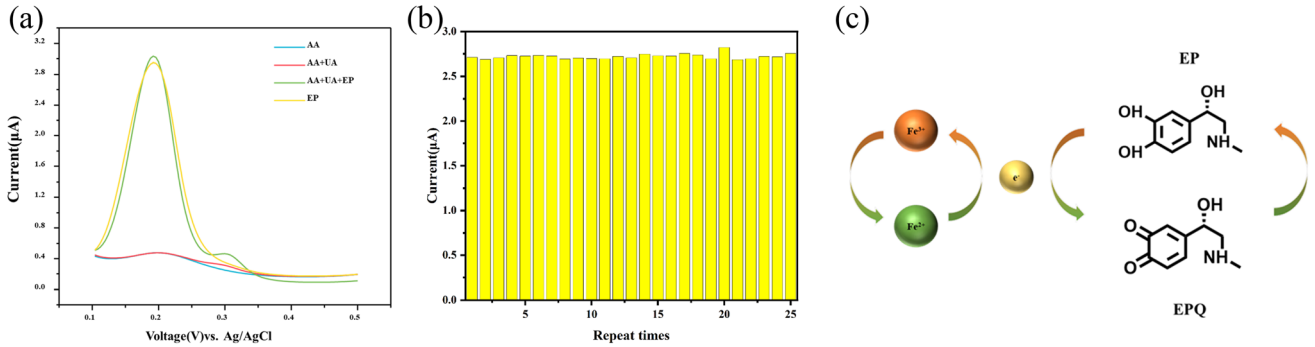

Fig. 4 (a) DPV response of $K_2Fe_4O_7$/GCE in 0.1 M PBS (pH = 7.4) containing 1 mM AA; 1 mM AA and 100 μM UA; 100 μM UA and 100 μM EP; 100 μM EP respectively. (b) Results of eight independent tests of $K_2Fe_4O_7$/GCE. (c) Brief detection mechanism.

signal remained stable, showing the sensor's suitability for EP detection.

Detection mechanism

$K_2Fe_4O_7$ has been demonstrated to be a viable material for electrochemical analysis. However, according to our previous research, the molecule cannot directly gain electrons on the electrode surface.[21] But $K_2Fe_4O_7$ has been shown to be a solid electrolyte,[22] which further illustrates that the valence state of elemental iron can undergo a reversible transition. Thus, we proposed a brief detection mechanism (Fig. 4(c)).

Conclusions

In summary, $K_2Fe_4O_7$ was investigated as an electrode modification material to detect EP efficiently. The response currents of the electrode display a linear increase proportional to the concentrations of EP from 2 μM to 260 μM, with a detection limit of 0.27 μM (S/N = 3). Additionally, $K_2Fe_4O_7$/GCE performs a high selectivity and stability. This electrochemical sensor provides another application of iron-based catalyst and offers a new choice in detecting EP.

Conflicts of interest

There are no conflicts to declare.

Acknowledgements

This work is supported financially by the State Key Laboratory of Inorganic Synthesis and Preparative Chemistry.

References

1 S. Immanuel and R. Sivasubramanian, *Bull. Mater. Sci.*, 2020, **43**, 79.
2 T. Tavana, M. A. Khalilzadeh, H. Karimi-Maleh, A. A. Ensafi, H. Beitollahi and D. Zareyee, *J. Mol. Liq.*, 2012, **168**, 69–74.
3 T. Thomas, R. J. Mascarenhas, O. J. D. Souza, S. Detriche, Z. Mekhalif and P. Martis, *Talanta*, 2014, **125**, 352–360.
4 D. M. Fouad and W. A. El-Said, *J. Nanomater.*, 2016, **2016**, 6194230.
5 C. Wang, F. X. Hu, X. C. Zou, Y. Q. Wang, Y. R. Ren and J. Tan, *Talanta*, 2022, **248**, 123621.
6 M. A. Fotopoulou and P. C. Ioannou, *Anal. Chim. Acta*, 2002, **462**, 179–185.
7 X. L. Zhu, P. N. Shaw and D. A. Barrett, *Anal. Chim. Acta*, 2003, **478**, 259–269.
8 Y. Y. Su, J. A. Wang and G. N. Chen, *Talanta*, 2005, **65**, 531–536.
9 T. Łuczak, *Electroanalysis*, 2009, **21**, 2557–2562.
10 M. D. Tezerjani, A. Benvidi, A. Dehghani Firouzabadi, M. Mazloum-Ardakani and A. Akbari, *Measurement*, 2017, **101**, 183–189.
11 F. Liu and X. Kan, *J. Electroanal. Chem.*, 2019, **836**, 182–189.
12 H. Yi, D. Zheng, C. Hu and S. Hu, *Electroanalysis*, 2008, **20**, 1143–1146.
13 M. Taleb, R. Ivanov, S. Bereznev, S. H. Kazemi and I. Hussainova, *J. Electroanal. Chem.*, 2018, **823**, 184–192.
14 L. Zou, Y. Li, S. Cao and B. Ye, *Talanta*, 2013, **117**, 333–337.
15 Y. Nishibayashi, *Dalton Trans.*, 2018, **47**, 11290–11297.
16 W. Zhang, J. Zheng, J. Shi, Z. Lin, Q. Huang, H. Zhang, C. Wei, J. Chen, S. Hu and A. Hao, *Anal. Chim. Acta*, 2015, **853**, 285–290.
17 Y. Huang, Y. Zhang, D. Liu, M. Li, Y. Yu, W. Yang and H. Li, *Talanta*, 2019, **201**, 511–518.
18 Y. Liu, W. Zhu, D. Wu and Q. Wei, *Measurement*, 2015, **60**, 1–5.
19 X. Ke, Z. Zhao, J. Huang, C. Liu, G. Huang, J. Tan, H. Zhu, Z. Xiao, X. Liu, Y. Mei and J. Chu, *ACS Appl. Mater. Interfaces*, 2023, **15**, 12005–12016.
20 W. Shan, X. Ma, G. Chen, F. Xu, H. Zhao, L. Dong, X. Yan, Z. Bi, L. Yu and M. Qiu, *J. Electrochem. Soc.*, 2023, **170**, 047514.
21 X. Sun, L. Zhang, X. Zhang, X. Liu, J. Jian, D. Kong, D. Zeng, H. Yuan and S. Feng, *Biosens. Bioelectron.*, 2020, **153**, 112045.
22 H. M. Yuan, H. Li, T. S. Zhang, G. H. Li, T. M. He, F. Du and S. H. Feng, *J. Mater. Chem. A*, 2018, **6**, 8413–8418.
23 M. Rafiee, L. Khalafi, F. Mousavi, F. Babaloii and F. Kalhori, *Electroanalysis*, 2017, **29**, 2004–2007.

24 S. Majdi, A. Jabbari, H. Heli and A. A. Moosavi-Movahedi, *Electrochim. Acta*, 2007, **52**, 4622–4629.
25 F. Fallah, M. R. Shishehbore and A. Sheibani, *Talanta*, 2023, **252**, 123776.
26 S. Renjini, P. Abraham, S. Aparna and V. A. Kumary, *J. Electrochem. Soc.*, 2019, **166**, B1321–B1329.
27 P. Shaikshavali, T. M. Reddy, T. V. Gopal, G. Venkataprasad, V. S. Kotakadi, V. N. Palakollu and R. Karpoormath, *Colloids Surf., A*, 2020, **584**, 124038.
28 P. Gopal, G. Narasimha and T. M. Reddy, *Process Biochem.*, 2020, **92**, 476–485.
29 L. V. da Silva, N. D. dos Santos, A. K. A. de Almeida, D. dos Santos, A. C. F. Santos, M. C. Franca, D. J. P. Lima, P. R. Lima and M. O. F. Goulart, *J. Electroanal. Chem.*, 2021, **881**, 114919.
30 M. F. Chen and X. Y. Ma, *Russ. J. Appl. Chem.*, 2014, **87**, 200–206.
31 B. Mekassa, M. Tessema, B. S. Chandravanshi, P. G. L. Baker and F. N. Muya, *J. Electroanal. Chem.*, 2017, **807**, 145–153.
32 M. L. Yola and N. Atar, *Composites, Part B*, 2019, **175**, 107113.